arXiv:1611.02366v1 [physics.optics] 8 Nov 2016

Laguerre-Gauss beam generation in IR and UV by subwavelength surface-relief gratings

Larissa Vertchenko[1], Evgeniy Shkondin[2], Radu Malureanu[3], and Carlos H. Monken[1]

[1]Departamento de Física, Universidade Federal de Minas Gerais, Caixa Postal 702, Belo Horizonte, MG 30161-970, Brazil
[2]Department of Photonics Engineering, Technical University of Denmark, Ørsteds Plads 343 DK-2800 Kgs. Lyngby, Denmark and Danish National Center for Micro and Nanofabrication (DANCHIP), DK-2800 Kongens Lyngby, Denmark
[3]Department of Photonics Engineering, Technical University of Denmark, Ørsteds Plads 343 DK-2800 Kgs. Lyngby, Denmark

November 9, 2016

Abstract

The angular momentum of light can be described by the states of spin angular momentum, associated with polarization, and orbital angular momentum, related to the helical structure of the wave front. Laguerre-Gaussian beams carry orbital angular momentum and their generation can be done by using an optical device known as q-plate. However, due to the usage of liquid crystals, these components may be restricted to operate in specific wavelengths and low power sources. Here we present the fabrication and characterization of q-plates made without liquid crystals, using processes of e-beam lithography, atomic layer depositions and dry etch techniques. We exploit the phenomenon of form birefringence to give rise to the spin-to-orbital angular momentum conversion. We demonstrate that these plates can generate beams with high quality for the UV and IR range, allowing them to interact with high power laser sources or inside laser cavities.

1 introduction

Q-plates are well known devices that couple spatial and polarization degrees of freedom of optical beams [1]. Due to this coupling, it is possible to exchange electromagnetic angular momentum between circular polarization modes

(spin angular momentum) and helical wavefront modes (orbital angular momentum) [2, 3]. The orbital angular momentum (OAM) eigenstates [4], such as the Laguerre-Gauss (LG) transverse modes [5], are characterized in the cylindrical coordinate system by the azimuthal phase factor $\exp(il\phi)$, where l is an integer and ϕ the azimuthal angle. These modes have many applications including fiber mode selection [6], optical tweezers and micromanipulation [7]. In the domain of quantum optics, LG beams carry an OAM of $l\hbar$ per photon [8] and define an infinite basis in Hilbert space that can be represented, along with the spin angular momentum states, in a higher-order Poincaré sphere [9].

In order to generate an helical phase front, which carries OAM, one must introduce a convenient polarization and position dependent phase shift $\delta(\sigma, \mathbf{r})$ on the beam cross section. Usually, this task is realized in a q-plate by a thin layer of liquid crystal whose molecules have their axes oriented along a certain pattern engraved on a glass surface [10]. For example, when a circularly polarized Gaussian beam passes through a q-plate with $\delta = \pi$ ($\delta = 0$) for linear polarization along the radial (azimuthal) direction, its polarization handedness is flipped and it acquires an OAM of $\pm 2\hbar$. This situation is illustrated in Fig. 1. The right value of δ is achieved by tuning the q-plate either thermally [11] or electrially [12, 13].

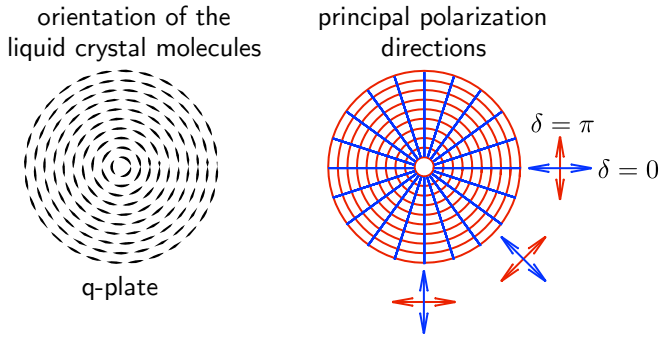

Figure 1: Example of a liquid crystal q-plate whose molecules are azimuthally oriented. The phase shifts are $\delta = 0$ for linear polarization along the radial direction and $\delta = \pi$ for linear polarization along the azimuthal direction.

Although the use of a liquid-crystal allows for relatively simple fabrication techniques [14], its absorption spectrum may set limits to the wavelength and power ranges that can be handled by the q-plate. These possible limitations can be circumvented by exploiting the phenomenon of form birefringence to fabricate q-plates with subwavelength surface relief gratings [15, 16, 17]. Due to technical difficulties in fabrication, subwavelength surface relief q-plates are in general limited to wavelengths of the order of $10\,\mu$m.

In this paper we exploit the phenomenon of form birefringence to fabricate a q-plate without the use of liquid crystals, capable of operating in a large wavelength range, from from IR to UV. The pattern formed by the structures was

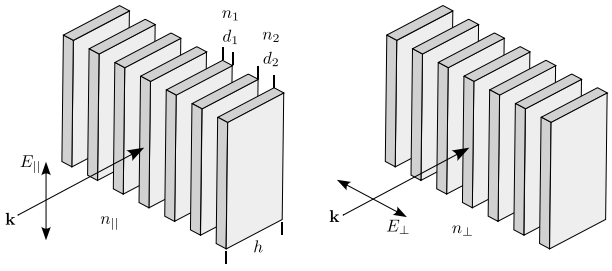

Figure 2: Form birefringence: a material of refractive index n_1 is arranged in a periodic nano structure with a filling factor f, and surrounded by a medium of refractive index n_2. Light linearly polarized in the directions parallel ($E_{||}$) and normal ($E_\perp$) to the interfaces will propagate with different velocities, corresponding to two different refractive indices $n_{||}$ and $n_\perp$.

chosen to be concentric circles of sub-wavelength grooves with the appropriate depth. This patern is able to generate LG beams of $l = \pm 2$ as explained below. After the fabrication process the q-plates were characterized using an asymmetric Mach-Zehnder interferometer and a CCD camera, showing the generation of high quality LG modes. We also investigated the interaction of the LG beams generated by q-plates with a nonlinear crystal, resulting in second harmonic generation (SHG), and how it affects the order and, consequently, the wave front of the incident modes. Starting from a pulsed Ti:Sapphire laser beam with an average power of 3.6 W, 120 ns pulses centred at $\lambda = 810$ nm at 80 MHz repetition rate, using different combinations of q-plates and SHG in sequence, we produced pulsed LG modes with $l = 2$, 4 and 6, centered at $\lambda = 405$ nm.

2 Form birefingence

Form birefringence may arise when sub-wavelength structures of different refractive indices are arranged with some order. According to the effective medium theory (EMT) [18], a periodic array of parallel slabs of thickness d_1 and refractive index n_1 separated by a gap d_2, embedded in a medium of refractive index n_2, as depicted in Fig. 2, will present a birefringence given by

$$\Delta n = n_{||} - n_\perp = \sqrt{f n_1^2 + (1-f) n_2^2} - \sqrt{\frac{f}{n_1^2} + \frac{1-f}{n_2^2}}, \qquad (1)$$

where $n_{||}$ and $n_\perp$ are the effective refractive indices corresponding to linear polarizations along the directions parallel and perpendicular to the slabs, respectively, and $f = d_1/(d_1 + d_2)$ is the filling factor.

Considering normal incidence and $n_2 = 1$ (air), diffraction effects will be absent when the structures have a maximum spatial period equivalent to $d_1 + d_2 = \Lambda = \lambda/n_1$ [19]. To achieve the desired phase retardation δ for our q-plates, the height h of the structures must be adjusted according to $h = \lambda\delta/(2\pi\Delta n)$.

3 Design and fabrication

The optical elements presented in this article were intended to work at the wavelengths of 810 nm in a pulsed laser source with an average power of 3.6 W and its second harmonic (405 nm). The material chosen to form the structures was titanium dioxide (TiO_2), which exhibits a refractive index of 2.52 at $\lambda = 810\,\text{nm}$ and 2.97 at $\lambda = 405\,\text{nm}$. In order to extinguish diffraction orders at 810 nm, the spatial period calculated was $\Lambda = 322\,\text{nm}$, which means that for $f = 0.5$ the trenches would have a width of 161 nm. With this period, some diffraction loss was expected at 405 nm. The height of the structure was chosen to be 300 nm, in order to have a conversion efficiency of the same order for both wavelengths. All the work has been carried out in class 100 cleanroom facility. The main steps of the fabrication process are shown in Fig.3.

A wafer of silicon dioxide (SiO_2) goes through RCA clean and low pressure chemical vapour deposition (LPCVD)(furnace from Tempress) based on SiH4 (silane) at 560°C to form a layer of 680 nm of amorphous silicon (Si)[Fig. 3(a)]. The back side of deposited Si was etched using sulphur hexafluoride (SF_6). In order to remove residues from the etching process it was performed oxygen plasma cleaning and RCA cleaning. A deposition of 150 nm of the resist CSAR was done followed by exposure to Electron Beam Lithography (EBL) (JEOL JBX-9500 Electron-beam)[Fig.3(b)] generating a mask of Si with concentric ring patterns. After development, the wafer was submitted to advanced silicon etch (ASE)[Fig.3(c)].

To form the trenches of the structures, a thin film of TiO_2 was deposited using the atomic layer deposition technique (ALD) in a hot-wall system (Picosun R200), working with 2000 cycles at 150°C [Fig.3(d)] [20]. The precursors used were titanium tetrachloride ($TiCl_4$) and H_2O (supplied by Strem Chemicals Equipment). The process was followed by Ar+ ion beam etching (IBE) on both sides of the wafer to remove excess[Fig.3(e)]. At the top most TiO_2 layer the physical sputtering of the sample using Ar+ ions was performed in order to get access to Si core. On the backside, the Ar+ ions were used to remove the deposited TiO_2[21].

Finally we performed a reactive ion etch on silicon, leaving only the TiO_2 structures. The final system comprehends a base of SiO_2 with nano-structures of TiO_2 on it [Fig.3(f)]. Figure 4a depicts an image taken from a scanning electron microscope (SEM) of the Si mask and Fig.4b, the final structures of TiO_2. Figure 5 shows the image of the system taken from an optical microscope.

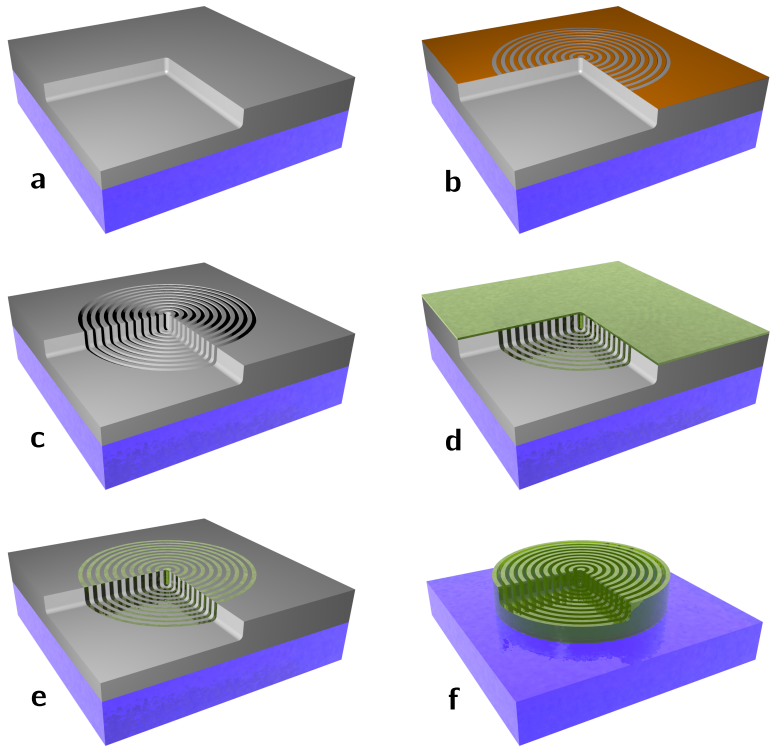

Figure 3: Scheme of fabrication flow. (a) Si deposited on SiO_2 by LPCVD process (only top part considered, sub sequential removal of the backside is not included). (b) E-beam lithography. (c) Advance silicon etching (ASE). (d) ALD of amorphous TiO_2. (e)Removal of TiO_2 by IBE (only top part considered) TiO_2 structures.(f) Isotropic SF_6 based RIE process and final structure.

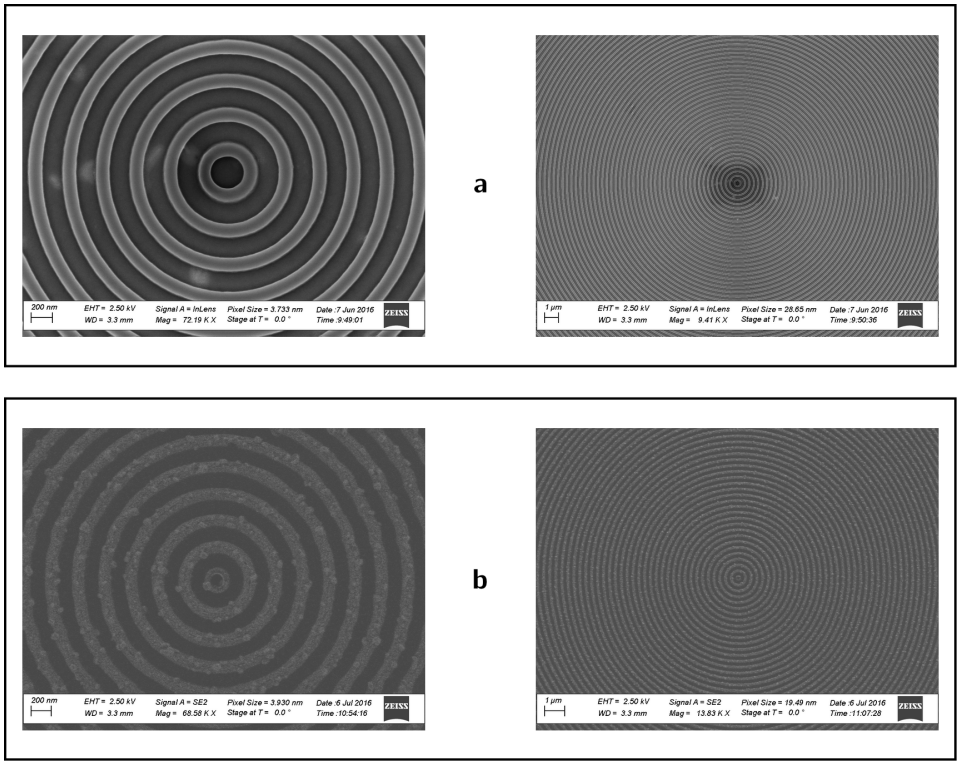

Figure 4: a) SEM image of the Si mask and b) TiO_2 structures

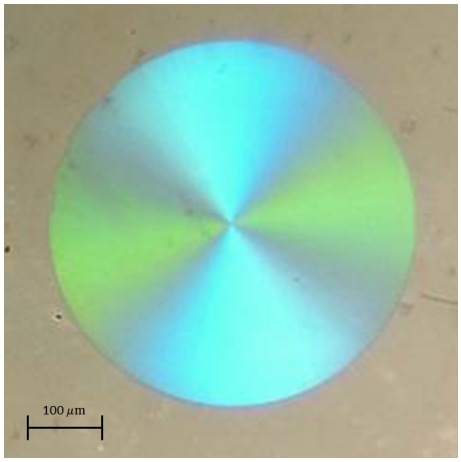

Figure 5: Image taken from an optical microscope

4 Higher order Laguerre-Gauss modes generation

The generation of a LG mode of $l = 2$ through a q-plate is achieved by considering the scheme shown in Fig.6. A Gaussian beam with horizontal polarization and $l = 0$ is converted to left circular polarization by a quarter wave plate ($\lambda/4$) and focused by the lens L on the q-plate. The outgoing wave is collimated by another lens (same as L) and filtered by another quarter wave plate and a polarizer (P) that transmits vertical polarization, which corresponds to the converted beam with right circular polarization. At the output of the polarizer we observe a Laguerre-Gaussian mode of $l = 2$. The intensity profile of the converted beam captured by a CCD (charge coupled device) camera is shown in Fig.7.

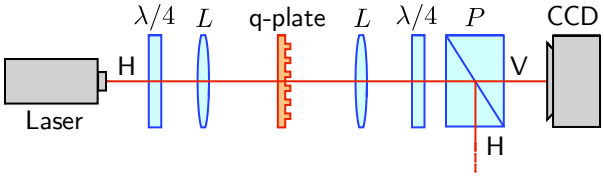

Figure 6: Setup for the generation of a Laguerre-Gauss mode using the fabricated q-plate

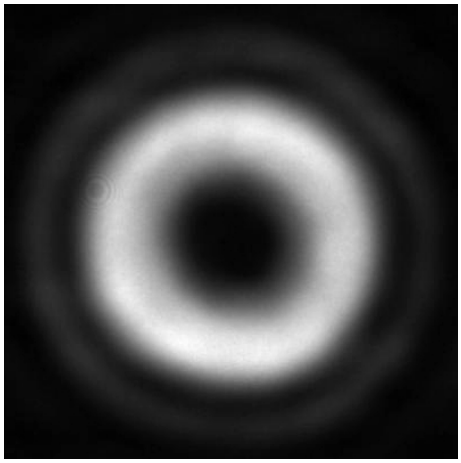

Figure 7: Intensity profile of the Laguerre-Gauss mode generated by the q-plate.

The conversion efficiency of our q-plates was defined as $\eta = I_V/(I_V + I_H)$, where I_V and I_H are the intensities transmitted and rejected by the polarizer P, as indicated in Fig. 6. The values measured were 0.45 for $\lambda = 810\,\text{nm}$ and 0.50 for $\lambda = 405\,\text{nm}$.

In order to demonstrate that the converted mode is indeed a LG with a helical wave front of $l = 2$, it is necessary to perform interferometric measurements. In our experiment we used an asymmetric Mach-Zehnder interferometer, which is able to interfere the transmitted beam with its mirror image, that has an inverted handedness profile due to an additional reflection inside the interferometer. The experimental set-up is illustrated in Fig. 8, and the simulated intensity profile compared with the one captured by the CCD camera is shown in Fig. 9.

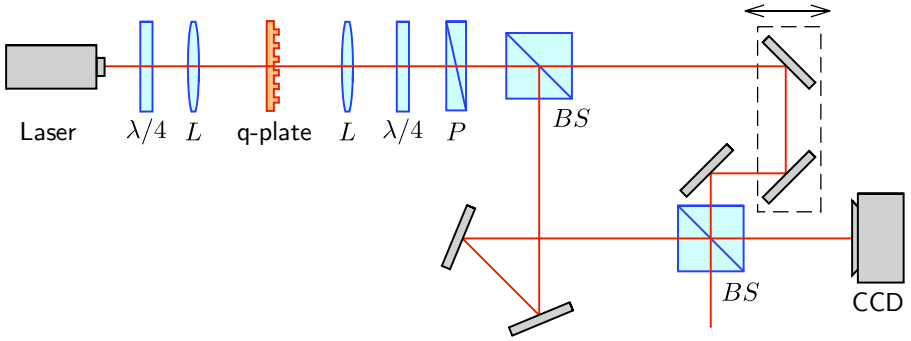

Figure 8: Setup with the asymmetric Mach-Zehnder interferometer

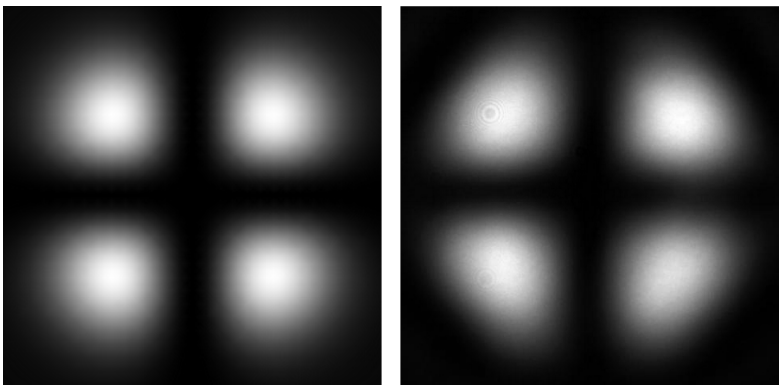

Figure 9: Simulated intensity profile of the interference between LG modes of $l = 2$ and $l = -2$ (Left), compared with the one captured by the CCD (Right)

Having a high quality LG mode generated, we then investigated the possibilities of second-harmonic generation (SHG) and combination of q-plates in order to generate modes with $l = 2$, 4 and 6.

It is known that the orbital angular momentum per photon is doubled in the process of second-harmonic generation (SHG) [22], resulting in a higher order mode of $2l$. The setup used, shown in Fig. 10, consists of a incident infrared

pulsed beam ($\lambda = 810\,\mathrm{nm}$) going through a BiB_3O_6 nonlinear crystal (BiBO), which produces a frequency-doubled ($\lambda = 405\,\mathrm{nm}$) beam. The asymmetric interferometer was positioned at the output to verify that the desired value of l was produced. If the q-plate QP_2 only is in place, an $l = 2$, $\lambda = 405\,\mathrm{nm}$ beam is obtained, just as in the infrared case discussed previously. When the q-plate QP_1 only is in place, an $l = 2$, $\lambda = 810\,\mathrm{nm}$ beam is produced and converted to an $l = 4$, $\lambda = 405\,\mathrm{nm}$ beam by SHG. Figure 11 shows the $l = 4$ Laguerre-Gauss mode intensity profile produced after SHG, captured by the CCD. One can observe that the mode is not as symmetric as the infrared one shown in Fig. 7, due to a slight astigmatism induced by the anisotropy of the nonlinear crystal. However through interferometric measurements shown in Fig. 12, we can guarantee that the OAM corresponding to $l = 4$ is still well defined.

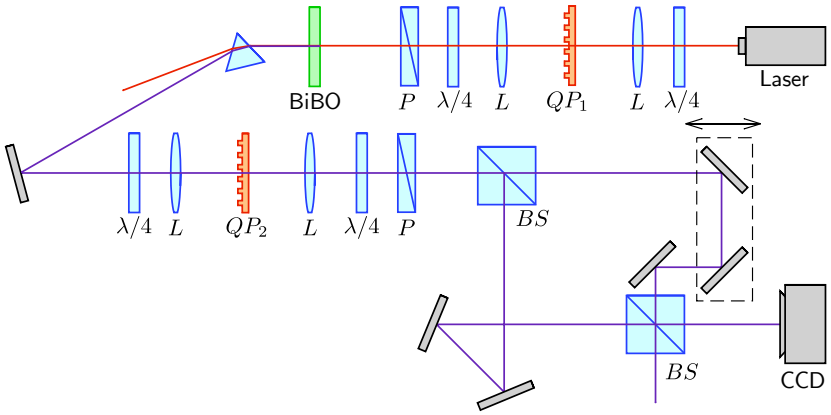

Figure 10: Set up for the generation of Laguerre-Gauss modes of $l = 2$, 4, 6.

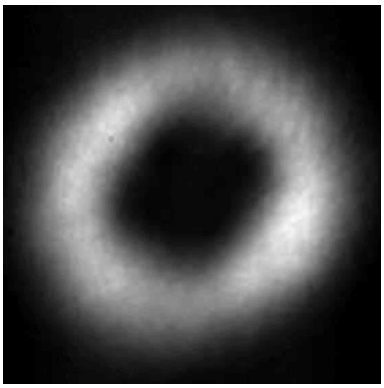

Figure 11: Intensity profile of the $l = 4$ Laguerre-Gauss mode after the SHG.

Finally, when both q-plates QP_1 and QP_2 are in place, an $l = 6$, $\lambda =$

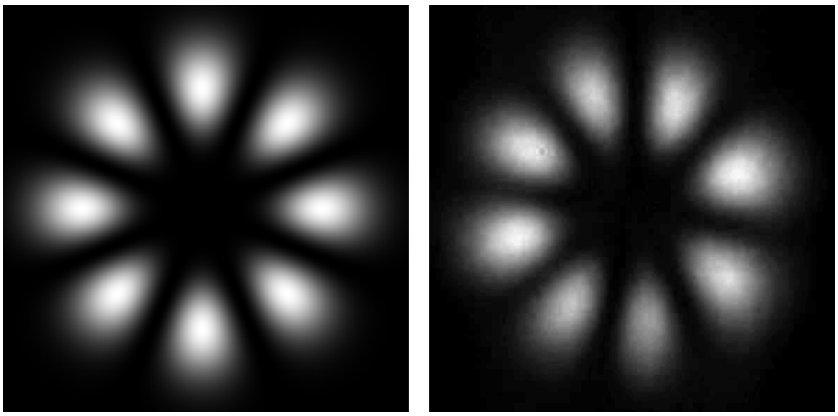

Figure 12: Simulated intensity profile of $l = 4$ (left) compared with the one captured by the CCD camera (right)

405 nm beam is obtained. The intensity profile captured by CCD after the interferometer is shown in Fig. 13.

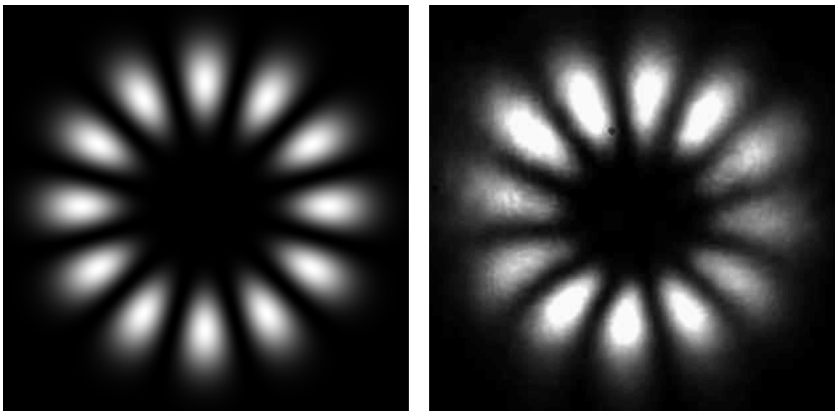

Figure 13: Simulated intensity profile for $l = 6$ (left) compared with the one captured by the CCD camera (right).

5 Discussion

We have demonstrated the generation of LG modes using q-plates exploring the phenomenon of form birefringence. The plates show high optical quality, operating with a high power pulsed laser source. Although we have used the same q-plate for 405 nm and 810 nm, they can be fabricated for the specific wavelengths, leading to higher conversion efficiencies. Our approach creates the possibility to easily fabricate phase plates with different patterns for any wavelength and without the necessity of liquid crystals. We have also proven the conservation of angular momentum during second-harmonic generation, producing beams with the orbital angular momentum doubled. By combining a set of q-plates and second harmonic generation, we were able to generate LG modes with $l = 2$, 4 and 6. The results presented in this paper may find applications in quantum optics and optical communications, due to the fact that we are capable of generating high quality Laguerre-Gauss modes of different orders, with no damage of the plates as a result of the laser power or the wavelength used. This feature is essential to form high dimension alphabet for optical communications and the prospect to insert these plates inside laser cavities.

Acknowledgements

We gratefully acknowledge financial support from the Brazilian agencies CNPq and FAPEMIG.

References

[1] L. Marrucci, C. Manzo, and D. Paparo, "Optical Spin-to-Orbital Angular Momentum Conversion in Inhomogeneous Anisotropic Media," Physical Review Letters **96**, 163905 (2006).

[2] M. Padgett and L. Allen, "Light with a twist in its tail," Contemporary Physics **41**, 275 (2000).

[3] L. Marrucci, "Rotating light with light: Generation of helical modes of light by spin-to-orbital angular momentum conversion in inhomogeneous liquid crystals," Proc. SPIE **6587**, 658708 (2007).

[4] S. Van Enk and G. Nienhuis, "Commutation Rules and Eigenvalues of Spin and Orbital Angular Momentum of Radiation Fields," Journal of Modern Optics **41**, 963 (1994).

[5] A. E. Siegman, *Lasers* (University Science Books, 1986).

[6] P. Gregg, M. Mirhosseini, A. Rubano, L. Marrucci, E. Karimi, R. Boyd, and S. Ramachandran, "Q-plates as higher order polarization controllers for orbital angular momentum modes of fiber," Optics letters **40**, 1729 (2015).

[7] A. M. Yao and M. J. Padgett, "Orbital angular momentum: origins, behavior and applications," Advances in Optics and Photonics **3**, 161 (2011).

[8] M. Padgett, "Light's twist," Proceedings of the Royal Society of London A: Mathematical, Physical and Engineering Sciences **470** (2014).

[9] D. Naidoo, F. S. Roux, A. Dudley, I. Litvin, B. Piccirillo, L. Marrucci, and A. Forbes, "Controlled generation of higher-order Poincaré sphere beams from a laser," Nature Photonics **10**, 327 (2016).

[10] L. Marrucci, "Generation of Helical Modes of Light by Spin-to-Orbital Angular Momentum Conversion in Inhomogeneous Liquid Crystals," Molecular Crystals and Liquid Crystals **488**, 148 (2008).

[11] E. Karimi, B. Piccirillo, E. Nagali, L. Marrucci, and E. Santamato, "Efficient generation and sorting of orbital angular momentum eigenmodes of light by thermally tuned q-plates," Applied Physics Letters **94**, 231124 (2009).

[12] E. Brasselet and C. Loussert, "Electrically controlled topological defects in liquid crystals as tunable spin-orbit encoders for photons," Optics Letters **36**, 719 (2011).

[13] S. Slussarenko, A. Murauski, T. Du, V. Chigrinov, L. Marrucci, and E. Santamato, "Tunable liquid crystal q-plates with arbitrary topological charge," Optics Express **19**, 4085 (2011).

[14] L. Marrucci, C. Manzo, and D. Paparo, "Pancharatnam-Berry phase optical elements for wave front shaping in the visible domain: Switchable helical mode generation," Applied Physics Letters **88**, 221102 (2006).

[15] G. Biener, A. Niv, V. Kleiner, and E. Hasman, "Formation of helical beams by use of Pancharatnam-Berry phase optical elements," Optics Letters **27**, 1875 (2002).

[16] A. Niv, G. Biener, V. Kleiner, and E. Hasman, "Spiral phase elements obtained by use of discrete space-variant subwavelength gratings," Optics Communications **251**, 306 (2005).

[17] C. H. Tsai, U. Levy, L. Pang, and Y. Fainman, "Form-birefringent space-variant inhomogeneous medium element for shaping point-spread functions," Applied Optics **45**, 1777 (2006).

[18] M. Born, E. Wolf, and A. Bhatia, *Principles of Optics: Electromagnetic Theory of Propagation, Interference and Diffraction of Light* (Cambridge University Press, 1999).

[19] D. H. Raguin and G. M. Morris, "Antireflection structured surfaces for the infrared spectral region," Applied Optics **32**, 1154 (1993).

[20] E. Shkondin, O. Takayama, J. M. Lindhard, P. V. Larsen, M. D. Mar, F. Jensen, and A. V. Lavrinenko, "Fabrication of high aspect ratio tio2 and al2o3 nanogratings by atomic layer deposition," Journal of Vacuum Science & Technology A **34**, 031605 (2016).

[21] Y. Huang, G. Pandraud, and P. M. Sarro, "The atomic layer deposition array defined by etch-back technique: A new method to fabricate tio2 nanopillars, nanotubes and nanochannel arrays," Nanotechnology **23**, 485306 (2012).

[22] J. Courtial, K. Dholakia, L. Allen, and M. Padgett, "Second-harmonic generation and the conservation of orbital angular momentum with high-order laguerre-gaussian modes," Physical Review A **56**, 4193 (1997).